Science of the Total Environment 447 (2013) 225–234

Contents lists available at SciVerse ScienceDirect

Science of the Total Environment

journal homepage: www.elsevier.com/locate/scitotenv

# Effects of environmental conditions on latex degradation in aquatic systems

Scott Lambert [a,b,*], Chris J. Sinclair [b], Emma L. Bradley [b], Alistair B.A. Boxall [a]

[a] Environment Department, University of York, Heslington, York, YO10 5DD, UK
[b] The Food and Environment Research Agency, Sand Hutton, York, YO41 1LZ, UK

## HIGHLIGHTS

- We characterised the degradation of latex in outdoor aquatic microcosms.
- Degradation rate was dependent on light and material thickness.
- Photooxidation is shown to be the primary degradation pathway.
- Degradation products include the formation of nanosized particles.
- Mass balance indicates that loses to the atmosphere occur.

## ARTICLE INFO

*Article history:*
Received 30 August 2012
Received in revised form 19 December 2012
Accepted 20 December 2012
Available online 4 February 2013

*Keywords:*
Polymers
Latex
Degradation
Nanoparticles
Photoxidation

## ABSTRACT

Following use polymer materials may be released to the natural environment distributed to various environmental compartments and may undergo a variety of mechanical and chemical weathering processes. This study characterised the degradation of a latex polymer of different thicknesses under a range of environmental conditions in outdoor microcosms. Samples were immersed in either demineralised water, artificial freshwater and marine water media and exposed for a period of 200–250 days with exposure starting at different times of the year. Effects of pH, agitation and the exclusion of light on degradation were also studied. At the end of the exposure period, recovery of polymer material ≥ 1.6 μm ranged from a low of 22.04% (±16.35, for the freshwater treatment at pH 5.5) to a high of 97.73% (±0.38, for the exclusion of light treatment). The disappearance of the bulk material corresponded to an increase in nanoparticles and dissolved organic material in the test media. Modelled degradation kinetics were characterised by multi-phasic degradation patterns and the results indicated degradation rate is affected by light intensity and polymer thickness. Mass balance analysis indicates that losses of volatile materials to the air compartment may also be occurring.



## 1. Introduction

The release of polymer materials (PMs) into the environment is recognised as an issue of worldwide concern (Barnes et al., 2009). A number of studies have demonstrated PMs to be a major component of litter on the ocean surface (Barnes and Milner, 2005; Barnes et al., 2010), on the seafloor (Galgani et al., 2000; Oigman-Pszczol and Creed, 2007; Stefatos et al., 1999) and on coastlines around the world (Bravo et al., 2009; Santos et al., 2009). Once in the environment PMs may be degraded by abiotic or biotic factors working together or in sequence (Agamuthu and Faizura, 2005; Krzan et al., 2006). Degradation of PMs could involve disintegration of the PM into increasingly smaller polymer fragments, including microscopic and nanosized particles; chemical transformation of the PM and polymer fragments; degradation of the PM and polymer fragments into non-polymer organic molecules; transformation/degradation of these non-polymer molecules into other compounds; and ultimate mineralisation to carbon dioxide and water. Due to the many degradation processes that occur, environmental systems receiving PMs will potentially be exposed to a complex mixture of the parent material, polymer fragments of different sizes and polymer degradation and transformation products. Each of these could be taken up by and affect aquatic and terrestrial organisms. For example, there is increasing concern over the impacts of nanoparticles on organisms as particle size is recognised as an important property in determining their interaction with living systems. Desai et al. (1997) showed that 100 nm sized particles of a polylactic polyglycolic acid co-polymer had a 10-fold higher intracellular uptake in an in-vitro cell culture when compared to 10 μm sized particles made of the same material. Nanoparticles have also been shown to produce cytotoxic, genotoxic, inflammatory and oxidative stress responses in mammalian and fish systems (Dhawan et al., 2011).

The majority of our current understanding on the processes influencing polymer degradation has been derived from artificial laboratory studies that investigate a single mechanism of degradation such as photodegradation (N. Nagai et al., 2005; Y. Nagai et al., 2005),

* Corresponding author at: Environment Department, University of York, Heslington, York, YO10 5DD, UK. Tel.: +44 7967332512.
*E-mail address:* scott.lambert@fera.gsi.gov.uk (S. Lambert).

0048-9697/$ – see front matter © 2013 Elsevier B.V. All rights reserved.
http://dx.doi.org/10.1016/j.scitotenv.2012.12.067

thermal degradation (Agostini et al., 2008; Cit et al., 2010), and biodegradation using microbial cultures (Cherian and Jayachandran, 2009; Cosgrove et al., 2007; Linos et al., 2000; Saad et al., 2010; Tsuchii et al., 1997). There is limited information on the degradation of polymers under environmentally relevant conditions where a number of degradation mechanisms occur at once and where information is available, the focus has been on understanding degradation in marine systems (O'Brine and Thompson, 2010; Rutkowska et al., 2002a,b; Sudhakar et al., 2007). These studies have tended to focus on weight loss, changes in tensile strength, breakdown of molecular structure and identification of specific microbial strains to utilise specific polymer types. The potential for PMs to form other chemical compounds and nano-sized particles has received little attention.

The aim of this work was therefore to characterise the degradation of a case study polymeric latex film under realistic conditions. To do this, outdoor microcosms were used so that the formation and subsequent degradation of the polymer transformation products could be monitored over time under natural cycles of sunlight and temperature. Experiments were initiated at different times of the year to cover different seasons and freshwater was used as the basic degradation medium. The specific objectives were to: i) explore the effects of season on the degradation rate of the latex film, ii) explore differences in degradation rates in freshwater and marine water, iii) investigate the importance of temperature and light for polymer degradation, iv) characterise molecular changes to the latex film during the degradation process, and v) characterise to what extent particles in the nanometer size range are formed following degradation of a polymer.

## 2. Methods

### 2.1. General study design

The degradation studies were undertaken using a latex film which is used in the manufacture of medical devices (0.08 mm thickness, provided by a leading UK manufacturer). For all studies, latex samples (approximately 25 $cm^2$) were placed individually into clear glass vessels (volume 250 ml) and spread out in 200 ml of test media. For each time point individual samples were established in triplicate and control samples, without latex, were also established. To expose the latex to natural cycles of sunlight and temperature, test vessels were then placed outdoors on a platform, under non-sterile conditions, and covered with a non ultra-violet filtering perspex sheet (B&Q, UK) to prevent flooding by rainfall. Evaporation was dealt with by regularly replacing lost water with the respective media, except for the marine water experiment where demineralised water was used to prevent the build-up of salts. Weather conditions for the entire study were recorded using a weather station located next to the experimental site (Delta-T Devices Ltd., UK).

#### 2.1.1. Semi-field degradation over different seasons

To understand the effects of season on the degradation of latex, two experiments were initiated at different times of the year: one in August 2010 and one in November 2010. The degradation medium used was demineralised water. For the summer study, samples were removed for analysis after 10, 20, 35, 50, 90, 120 and 250 days of exposure and for the winter study, samples were removed after 30, 60, 90, 120, 150 and 200 days. A water/sediment system was also investigated during these time periods but the results were inconclusive so will not be reported here.

#### 2.1.2. Importance of selected environmental variables and thickness on latex degradation

To assess the effects of different environmental variables on latex degradation, a series of studies were undertaken in June 2011 using an artificial freshwater media (pH 7.9; containing $CaCl_2$ 294 mg/l; $MgSO_4$ 123.25 mg/l; $NaHCO_3$ 64.75 mg/l and KCl 5.75 mg/l). The variables investigated were; an additional pH value (pH 5.5); presence/absence of sunlight; and water movement. Studies were also performed using artificial marine water (Red Sea Salt mix, Red Sea Aquatics Ltd., UK, batch number 26 04 0915; pH 8.4), and a thicker latex film (1.5 mm). Media pH was adjusted using either NaOH or HCl accordingly. The exclusion of light was achieved by covering the test vessels with foil and the effect of water movement was simulated by shaking the relevant vessels once a week for 16 h at 80 rpm. For all of these manipulations a more rigorous sampling regime was applied with samples being removed and taken for analysis after 1, 3, 7, 14, 28, 56, 112 and 200 days of exposure. Throughout the study pH was recorded (see Supporting information Table 1).

### 2.2. Analytical methods

#### 2.2.1. Weight loss

Upon collection, samples were filtered under vacuum using pre-dried and weighed, 1.6 μm pore diameter, glass fibre filter papers (Whatman, UK). The filter papers were then dried at 40 °C to a constant weight and the weight recorded. A sample (20 ml) of the filtered test media was taken at this stage and stored at 5 °C for characterization in terms of nanoparticle concentration and size distribution and dissolved organic carbon (DOC) concentration. For material from the marine media, it was necessary to wash the salts off the filtered sample. To do this, samples were immersed in demineralised water for 24 h and filtered. This process was repeated until a constant weight was measured. After weighing, latex samples were kept in the fridge until the chemical functionality of the latex sample could be assessed.

#### 2.2.2. Changes in chemical functionality

Changes in chemical functionality of the latex samples were characterised using Fourier Transform Infra-Red spectroscopy (FTIR). The infra-red absorption spectra of the filtered latex samples were measured using an ATR (Attenuated Total Reflection)-FTIR. ATR makes use of an evanescent wave to collect the absorption spectrum of a studied sample as radiation is passed through a crystal at an angle in which total reflection occurs on the top surface where the sample is located. The FTIR spectra were recorded using a Bruker spectrometer model Vertex 70 (Bruker, Germany) in the 400–4000 $cm^{-1}$ wave number range. All spectra were the average of 16 scans recorded at a resolution of 4 $cm^{-1}$ and peak height was used to represent the IR intensity, which is expressed as absorbance.

#### 2.2.3. Particle analysis

Nanoparticle tracking analysis (NTA) was used to determine the number and size distribution of particles in the size range 30 nm to 2000 nm. Analysis was performed using a NanoSight LM 10 (NanoSight Ltd., UK). To characterise each individual sample and control in a representative manner, nine video images of each sample were taken. The focus of the camera was judged by eye and was adjusted so the majority of particles on the screen were in focus at the start of video capturing. Video image length was set at 60 s and all images were taken at room temperature. The processing of video images was performed using NTA 2.2 software. The detection threshold was set to automatic; this determines the minimum grey scale value of any particle in the image necessary for it to qualify as a particle to be tracked. A blur (smoothing setting) of $5 \times 5$ was then used following the recommendation in the operating manual that if automatic threshold detection is used, the blur setting should be increased by one level higher than normally used. The minimum expected particle size was set at 30 nm for all samples due to the unknown nature of the samples being analysed. The minimum track length, which defines the minimum number of steps a particle must take before its size is calculated and included in the analysis, was set to automatic allowing the software to calculate this based on the particles in the video. To verify that the filtering process was not affecting the distribution profiles, a mixture of mono-dispersed

500 nm and 1000 nm (12:1 ratio) polystyrene beads were characterised, then filtered through a 1.6 μm filter paper and then characterised again (Supplementary data Fig. 1). This shows the presence of two distinct size populations indicating that NanoSight is indeed suitable for polydispered samples and the filtering process has not interfered with the sample.

*2.2.4. Dissolved organic carbon analysis*

Degradation media were analysed with a LiquiTOC combustion analyzer (Elementar, Germany). Subsamples of the degradation media were diluted 10-fold with demineralised water to bring them within the calibration range. The diluted sample was then filtered using a 0.45 μm glass fibre filter paper (Whatman, UK) to separate the dissolved fraction from the solid fraction. A range of potassium hydrogen phthalate and sodium carbonate standards (1–50 mg/l) was used for making a standard curve from which DOC was calculated. Results for the latex treatments were corrected using the corresponding control DOC values.

*2.3. Data analysis*

*2.3.1. Degradation rate and modelling approach*

Degradation rates were calculated using a series of models that describe bi-phasic degradation (FOCUS, 2006). The results for the summer and winter experiments were best described by a hockey-stick model which assumes degradation initially occurs according to first-order kinetics which is described by a constant fractional rate of degradation ($k_1$) (Eq. (1)). Then at a certain point in time, known as the breakpoint, the rate constant changes to a different value ($k_2$) that declines with time (Eq. (2)).

$$M = M_0 e^{-k_1 t} \text{ for } t \le t_b \quad (1)$$

$$M = M_0 e^{-k_1 t_b} e^{-k_2 (t - t_b)} \text{ for } t > t_b \quad (2)$$

Where: M is the mass at time t; $M_0$ is the mass at the start of the study; $k_1$ is the rate constant for $t \le t_b$, $k_2$ is the rate constant for $t > t_b$, and $t_b$ is the time at which the constant changes.

The results for the second set of experiments appeared to be multi-phasic in nature as an increase in weight was seen at the beginning of the exposure period. To include this phase in the modelling process an exponential growth equation was fitted to this part of the measured data (Eq. (3)). Then at the point in time where weight loss starts to occur a breakpoint was applied and a revised version of a bi-exponential model (described as the sum of two first order equations (FOCUS, 2006)) was used to describe the remaining measured data (Eq. (4)).

$$M = M_0 e^{k_1 t} \text{ for } t \le t_b \quad (3)$$

$$M = M_1 e^{-k_2 (t - t_b)} + M_2 e^{-k_3 (t - t_b)} \text{ for } t > t_b \quad (4)$$

where $M_1$ is the amount of material applied to compartment 1 at time $t = breakpoint$, $M_2$ is the amount of material applied to compartment 2 at time $t = breakpoint$, $k_2$ is the rate constant in compartment 1 and $k_3$ is the rate constant in compartment 2. $M_1 + M_2$ must be equal to the weight of material at which the breakpoint is applied.

Model parameters were fitted by applying a trial and error approach (see Supplementary data, Table 2). Estimation of the time taken for 50% ($DT_{50}$) of the latex to degrade for the summer and winter treatments was derived from Eqs. (5) and (6). Model fits for the remaining treatments were derived from a modified version of a bi-exponential model, as there is no analytical equation to calculate degradation endpoints for this model, $DT_{50}$ values were derived from a table of calculated concentrations. Measurements used to assess goodness of fit for the optimised parameters were carried out using, sum of square residuals (SSRes), root mean square error (RMSE), chi-square test, model error and coefficient of determination ($r^2$ value) (Table 1); descriptions for these indices can be found in the FOCUS (2006) guidance document.

$$DT_x = \frac{1}{k_1} \ln\left(\frac{M_0}{M}\right) \text{ if } DT_x \le t_b \quad (5)$$

$$DT_x = t_b + \frac{1}{k_2} \ln\left(\frac{M_0}{M}\right) - \left(\frac{k_1}{k_2}\right) \text{ if } DT_x > t_b \quad (6)$$

*2.3.2. Relating degradation of parent material to weather parameters*

The weather data was used to estimate the amount of solar radiation (MJ $m^{-2}$) responsible per unit of degradation. This was achieved by calculating the difference in weight loss between consecutive time points and dividing through the amount of solar radiation received between sampling intervals; from this an overall average was determined. Sampling intervals with measured weight gain were excluded with calculations adjusted appropriately.

*2.3.3. Calculation of particle size distribution and particle mass*

To determine the particle size distribution in the samples that had contained latex, data on the particle size distribution and number concentration of the equivalent control treatment was subtracted from the treated sample data. This was corrected for the presence of any naturally occurring particles and particles that may have entered into the sample during the filtering process. The mass of particles present was estimated using the distribution data by calculating the volume of particles present in the sample (Eq. (7)) and then multiplying by the density of the solid which was taken to be 920 mg/$cm^3$ for polyisoprene (Eq. (8)). It should be noted that for this calculation it was assumed all particles were solid spheres (Gillespie et al., 2011).

$$\text{Volume} = \frac{\pi}{6} d^3(\text{cm}) \times \text{concentration}(\text{no.particles/ml}) \quad (7)$$

$$\text{Mass}(\text{mg/ml}) = \text{Volume} \times \rho \quad (8)$$

*2.3.4. Mass balance*

To assess losses of the latex to the atmosphere (e.g. through mineralisation of the polymer to $CO_2$ and $H_2O$ or volatilisation of organic transformation products or additives), a mass balance analysis was performed using the weight of material collected on the 1.6 μm filter paper, the DOC concentration (corrected for controls) and the mass of particles in the filtered media above 450 nm (particles below 450 nm were excluded as the mass of particles below 450 nm will be included in the DOC measurements). The combined weight was then compared to the material starting weight.

*2.3.5. Statistical analysis*

The generated datasets were identified as either non-normally distributed or of unequal variance using Kolmogorov–Smirnov test. Therefore, overall differences between treatments were evaluated using Friedman Repeated Measures ANOVA on Ranks. All statistical tests were followed by a post-hoc Tukey multiple comparisons test applied to the different combinations. Stepwise regression was used to identify which of mean temperature (°C) or mean intensity of solar radiation (MJ $m^{-2}$) each sampling interval received during its exposure, best describes degradation rate for each treatment investigated. All statistical tests were performed using SigmaPlot version 12 and a 95% significance level.

**Table 1**
Statistical indices derived for modelling of weight loss and values derived for explaining sunlight intensity as the driving factor.

| | Summer 2010 | Winter 2010 | Freshwater | Lower pH | With movement | Marine water |
|---|---|---|---|---|---|---|
| *Statistical indices* | | | | | | |
| $DT_{50}$ | 38.51 | 145.04 | 158 | 75.5 | 220 | 87 |
| SSRes | 368.43 | 32.79 | 59.3 | 158.39 | 80.59 | 240.17 |
| RMSE | 3.26 | 1.43 | 1.46 | 2.01 | 1.60 | 1.56 |
| $\chi^2$ (tabulated $\chi^2$) | 8.75 (9.49) | 0.92 (7.81) | 0.83 (5.99) | 5.25 (5.99) | 1.24 (5.99) | 4.74 (5.99) |
| Model error | 10.96 | 2.69 | 3.16 | 6.49 | 4.29 | 7.55 |
| $r^2$ | 0.91 | 0.98 | 0.90 | 0.94 | 0.88 | 0.93 |
| Sunlight intensity as a predictor for mass loss | $r^2=0.60$ ($p=0.002$) | | $r^2=0.87$ ($p=0.001$) | $r^2=0.81$ ($p=0.002$) | $r^2=0.74$ ($p=0.006$) | $r^2=0.87$ ($p=0.001$) |
| MJ $m^{-2}$ responsible for 1% weight loss* | 13.65 (±5.75) | 14.05 (±5.03) | 36.64 (±20.82) | 30.42 (±23.29) | 36.22 (±21.05) | 29.85 (±13.56) |

*$DT_{50}$* estimated time for 50% of the latex to degrade; *SSRes* Sum of square residuals; *RMSE* Root mean square error.
* Thicker material = 144.33 (23.34).

## 3. Results and discussion

### 3.1. Seasonal effects on degradation rate

The effect of season on degradation rate was pronounced. When exposure was initiated in August, latex samples started to disintegrate within 10 d, compared to the study initiated in November where degradation was negligible until the onset of spring (Fig. 1). The breakpoint ($t_b$) at which the second rate constant is used to describe the degradation kinetics, for the summer treatment, was modelled as 44 d. Over this 44 d period samples were exposed to an average daily temperature of 13.9 °C and a total of 421.01 MJ $m^{-2}$ of solar radiation was received; at the end of this treatment material recovery was 19.65% (±1.62).

The breakpoint for the winter treatment was modelled as 105 d, over which samples were exposed to a lower average daily temperature of 2.18 °C and received far less solar radiation (184.79 MJ $m^{-2}$); material recovery for this treatment after 200 d was 17.12% (±6.25). The total solar radiation received at the study site over the duration of each treatment was 1188 MJ $m^{-2}$ for the summer treatment and 1172 MJ $m^{-2}$ for the winter treatment. Solar radiation was identified as the weather variable that best described the seasonal effect on weight loss, with similar solar intensities responsible for one percent weight loss (Table 1). Previous studies have also demonstrated the enhanced degradation of polyethylene films when exposed to increased levels of sunlight intensity and higher temperatures in summer seasons (Al-Salem, 2009).

### 3.2. Effects of environmental conditions and polymer thickness on degradation of latex

When the effects of a range of environmental conditions on degradation were assessed over 200 d (Fig. 1) fastest degradation was seen in the lower pH media ($DT_{50}=75$ d), this was followed by the marine water treatment ($DT_{50}=87$ d) and the higher pH freshwater treatment ($DT_{50}=158$ d) (Table 1). Samples subjected to water movement gave a much longer $DT_{50}$ (220 d). The use of movement appeared to cause any fragmented particles to congeal, reducing the impacts of weathering. Limited degradation was seen in the samples where sunlight was excluded and in the thicker polymer samples, with material recovery after 200 d measured at 97.73% (±0.38) and 88.57% (±4.39) respectively; therefore it was not possible to model the degradation kinetics for these treatments. Overall, differences in degradation rate between these six treatments were identified ($\chi^2=12.762$, $p=0.026$); however, post-hoc analysis indicates only the thicker material and exclusion of light treatments to be significantly different from the other treatments.

The total solar radiation and average daily temperature received at the study site over the duration of this experimental period was 1651 MJ $m^{-2}$ and 12.22 °C respectively. Solar radiation was again identified as the weather variable that best described weight loss under each degradation scenario (Table 1). The corresponding sunlight intensities responsible for one percent degradation ranged from 30.42 MJ $m^{-2}$ for the lower pH treatment to 144.33 MJ $m^{-2}$ for the thicker material treatment (Table 1). Other studies have also demonstrated solar radiation as the driving variable for the rate of polymer degradation. Saad et al. (2010) investigated the effect of ultra violet (UV) radiation on the biodegradation rate of polyhydroxybutyrate (PHB) films 0.1–0.12 mm thickness, and found samples exposed to 9 h UV radiation had ~52% weight loss after 28 days soil burial compared to ~32% weight loss for samples with no pre UV exposure. Polyethylene samples (0.08 mm thickness) immersed in the Baltic Sea for 20 months were also found to have no measureable weight changes because of the lack of sunlight in this environment (Rutkowska et al., 2002a).

### 3.3. Changes in chemical functionality of the latex over time

FTIR spectra of unexposed latex contained several peaks characteristic of vibration modes attributed to *cis*-1,4 polyisoprene (Agostini et al., 2008; Nor and Ebdon, 2000). Absorption bands were observed at 2960 $cm^{-1}$ which arise from C–H asymmetric stretching in $CH_3$ groups and a strong absorption band was also seen at 1450 $cm^{-1}$ characteristic of angular deformation of $-CH_2$-groups (Nor and Ebdon, 2000). Exposure to natural sunlight and temperatures resulted in a weakening of these absorbance bands ($\chi^2=27.571$, $p<0.001$ and $F=22.143$, $p<0.001$ respectively), but only treatments where sunlight was excluded and a thick material used were significantly different from other treatments.

The observed weakening of characteristic absorbance bands was accompanied by the formation of a broad OH peak in the region 3000–3600 $cm^{-1}$ and a low intensity CO band at 1715 $cm^{-1}$ (Fig. 2). OH and CO groups are oxy-generated products that attach themselves to polymer molecules and are formed by photo-oxidation processes (Albertsson et al., 1987). In the excluding light treatment these functional groups were only observed at very low absorbencies and were shown to be significantly different to other treatments ($\chi^2=31.286$, $p<0.001$ and $\chi^2=26$, $p<0.001$ respectively).

Under ambient conditions, photo-degradation is considered one of the primary sources of damage for polymeric materials (Klemchuk, 1990; Lucas et al., 2008). The lack of change observed in the FTIR spectra when light is excluded indicates photo-oxidation as the major pathway involved in degradation process. A possible mechanism for the photodegradation of latex is shown in Fig. 3. This initially involves the light-driven oxidative scission of the C=C bond in the *cis*-1,4 polyisoprene chain as described by Tsuchii et al. (1985) (Fig. 3, structure I) forming end chain CO groups. The formation of OH end groups (structure VII) is preceded by the UV induced change in the chemical structure of the latex molecules which occurs through free radical intermediates (structure III). These reactive intermediates are formed when the latex absorbs light and oxygen which easily undergo photolysis into intermediate hydroperoxide groups (structure IV) as described by Mailhot et al. (2000) and Kaczmarek et al. (2007)

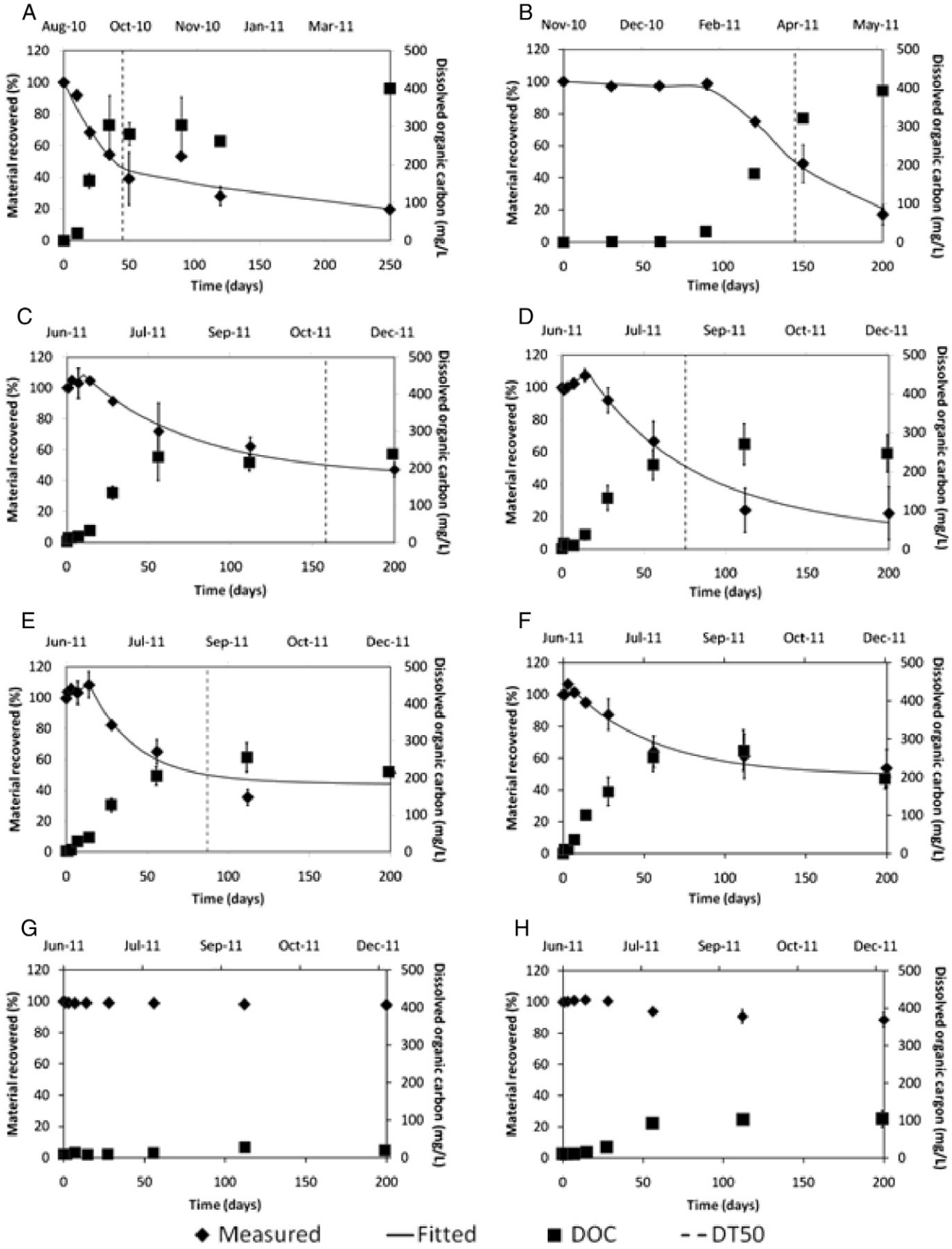


**Fig. 1.** Degradation of latex over time in, A) August 2010 treatment; B) November 2010 treatment; C) artificial freshwater (pH 7.9); D) artificial freshwater (pH 5.5); E) artificial marine water; F) simulated water movement; G) absence of light; and H) the thicker latex sample. Diamond shaped data points represent mean material recovery of three replicate measures; the solid line dissecting these data points represents the best fit model obtained using the FOCUS approach; the vertical dashed line represents the point at which 50% degradation is reached and the squares represent dissolved organic carbon. For all plots error bars displayed were obtained by the standard deviation of the different measurements for each sample; bars where not visible fall within the symbols.

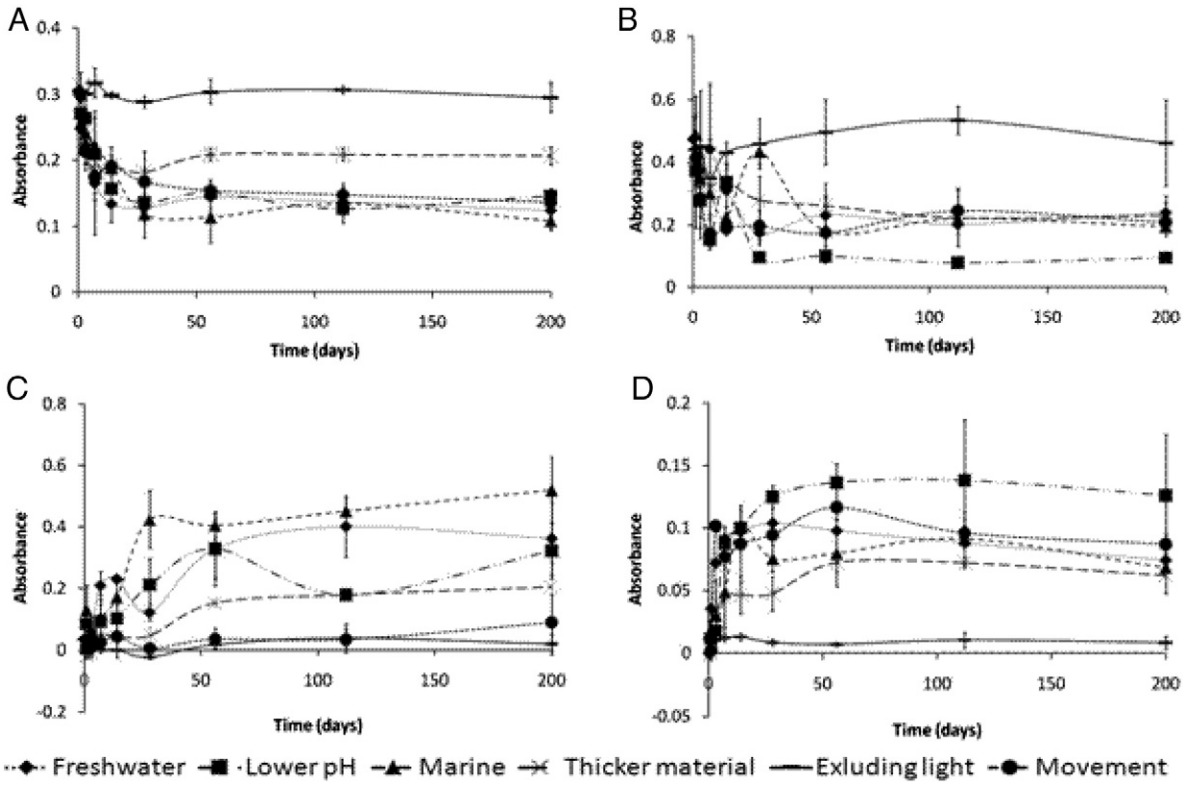


**Fig. 2.** Changes in FTIR-ATR peak intensities during exposure to natural cycles of sunlight and temperature at, A) 2960 $cm^{-1}$; B) 1450 $cm^{-1}$; C) 3000–3600 $cm^{-1}$ and D) 1715 $cm^{-1}$. Diamonds = freshwater treatment; squares = lower pH treatment; triangles = marine water treatment; stars = thicker material; circles = simulation of movement; solid line = exclusion of light.

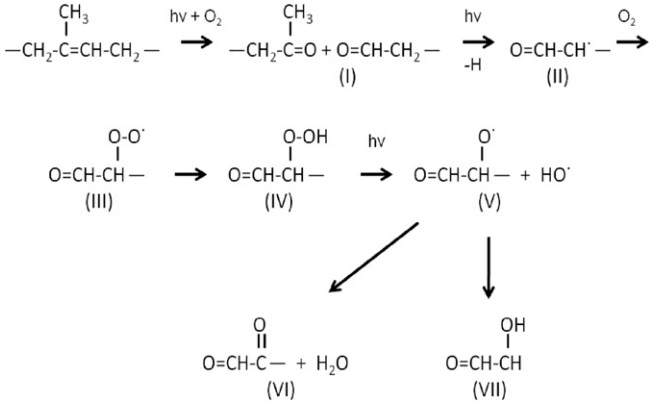


**Fig. 3.** Proposed route for breakdown of latex in the aquatic environment.

in photo-degradation experiments of polystyrene and poly(ethylene oxide) respectively. Further CO groups may also be produced by photo-oxidation processes (structure VI) (Kaczmarek et al., 2007). The appearance of CO and OH groups is also noted by Agostini et al. (thermal degradation) and Riyajan et al. (2003) in the biodegradation of natural rubber.

### 3.4. Formation of nanoparticles

NTA was used to characterise both the concentration and size distribution of particles < 1.6 μm formed during the degradation of latex (Fig. 4). Previous studies have shown this technique to be suitable for characterisation of samples with heterogeneous distributions of nanoparticles as it does not give bias towards larger particles (Filipe et al., 2010; Montes-Burgos et al., 2010). The results show that particles < 1.6 μm were formed from the latex over the course of the exposure period when compared to concentrations in the controls. After 200 d the concentration of particles in the freshwater treatment was $3.30 \times 10^8$/ml (±0.79), this compares to $0.2 \times 10^8$/ml (±0.13) in the control for the same time point (Fig. 6). Particles in the control samples most likely originate from atmospheric dust entering the sample during the exposure period.

The highest concentration of particles after 200 d was measured for samples taken from the vessels where water movement was simulated and from the thicker latex treatment ($4.89 \times 10^8$/ml ± 1.28 and $4.80 \times 10^8$/ml ± 1.38, respectively), even though overall degradation rate of the latex, based on weight loss, was lower in these two treatments than the other treatments. Overall differences in particle concentrations in the second set of experiments were identified ($\chi^2 = 256.359$, $p < 0.001$), with exclusion of light and marine water treatments found to be significantly different from the other treatments even though the marine media experiment had comparable weight loss to the experiments based in freshwater media.

Mean particle diameter was the same across exposure treatments (Fig. 4; $\chi^2 = 9.929$, $p > 0.05$). After 200 d mean particle diameter ranged from 196.52 nm (±89.48) in the freshwater treatment to 207.33 nm (±100.29) in the lower pH treatment. Overall, the size of particles formed was mainly in the 100–400 nm range, with few larger particles (>400 nm) being measured. One possible explanation is that larger particles precipitate over time and only become re-suspended when they themselves further breakdown or they could potentially aggregate with time and therefore be caught by the filtering process.

The mass of latex particles present in the test media was also estimated, based on the particle size distribution and number concentration, and was generally seen to increases in line with particle concentration. The largest mass of particles present after 200 d was 3.83 μg/ml (±0.29) in the lower pH scenario, which accounts for

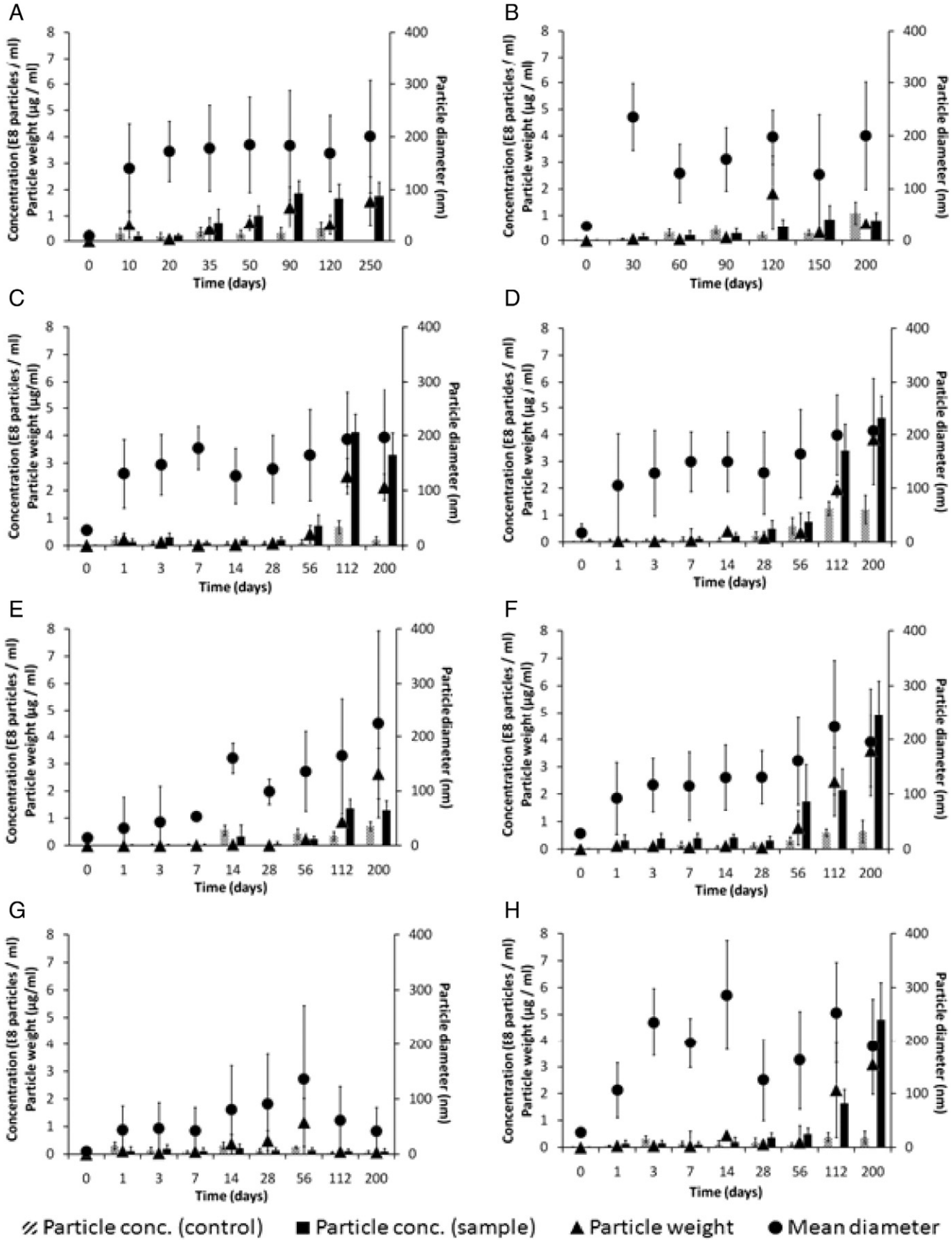


**Fig. 4.** Characterisation if nanosized particles formed during the degradation of latex in, A) August 2010 treatment; B) November 2010 treatment; C) artificial freshwater (pH 7.9); D) artificial freshwater (pH 5.5); E) artificial marine water; F) simulated water movement; G) absence of light; and H) a thicker latex sample. Solid bars represent particle concentration in the sample filtrate; bars with diagonal lines represent particle concentration in the controls; circles represent mean particle concentration in the samples and triangles represent particle weight. Error bars displayed were obtained by the standard deviation of the different measurements for each sample.

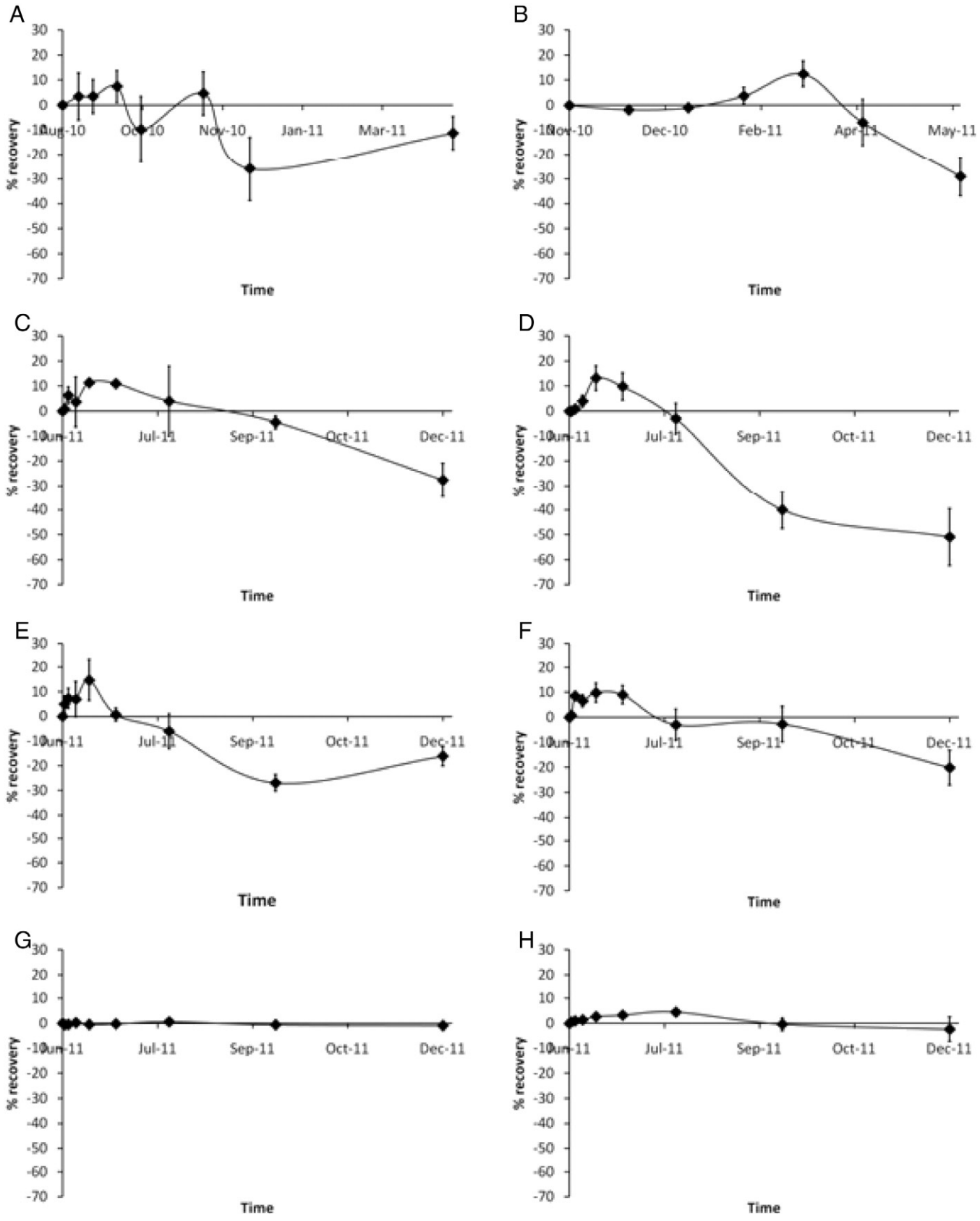


**Fig. 5.** Changes in the mass balance for the degradation of latex during exposure to natural cycles of sunlight and temperature in, A) August 2010 treatment; B) November 2010 treatment; C) artificial freshwater (pH 7.9); D) artificial freshwater (pH 5.5); E) artificial marine water; F) simulated water movement; G) absence of light; and H) a thicker latex sample.

0.54% (±0.06) of the material starting weight; this compares to a mass of 2.13 μg/ml (±0.48) after 200 d in the freshwater experiment, which accounts for 0.3% (±0.06) of the material starting weight.

### 3.5. DOC

An increase in the formation of DOC over time was observed for all treatments, with the exception of the vessels where sunlight was excluded (Fig. 1). The formation of DOC was closely related to the latex weight loss results with the faster periods of latex degradation corresponding with the rapid increase in DOC levels. Slower phases of degradation were associated with a stabilisation in measured DOC levels and can be attributed to the reduced sunlight intensities experienced throughout the autumn and winter months. DOC formation in the treatment where light was excluded and in the thick latex treatment was significantly lower than in all other treatments ($\chi^2 = 66.907$, $p < 0.001$).

### 3.6. Mass balance

Data from the weight loss, particle and DOC measurements were combined to determine whether the mass loss of latex could be explained by particle formation and formation of soluble organic transformation products alone (Fig. 5). For the exclusion of light and thicker material treatments it was possible to develop a mass balance for all sampling points, however, this was not the case for the remaining treatments. For these remaining six treatments an increase in total mass was observed as the latex starts to break apart and degrade. The mass increases may be due to a combination of processes which include the formation of microbial biomass on the latex, as biodegradation is a mechanism of degradation for some polymers (Linos et al., 2000). As microbiological analysis was not undertaken mass increase due to absorption of oxygen cannot be ruled out. The addition of oxygen due to photo-oxidation processes may also contribute to increases in mass. As time progresses it was not possible to develop a full mass balanced indicating that other loss mechanisms might be occurring. This might be explained by volatilization processes that come into effect as the latex degrades (Agostini et al., 2008). The decreasing absorbance in the IR spectra indicates degradation of the macromolecules occurs. This degradation could be due to chain breakage as proposed in Fig. 3 coupled with the evolution of low-molecular volatile products.

## 4. Conclusion

This study has attempted as far as possible to mimic field conditions. Modelled degradation kinetics are characterised by multi-phasic degradation patterns and degradation rate is affected by sunlight intensity and polymer thickness. The degradation mechanism is that of photo induced weakening of the polymer matrix as indicated by the FTIR analysis, coupled with the formation of oxidation products; these structural changes then result in the disintegration of the latex film.

The major finding of this study was to identify and quantify the formation of particles in the nanosize range as well as dissolved organic compounds. The mass balance analysis also indicates that losses of volatile materials to the air compartment may also occur. The results are significant as they show that receiving environments are potentially exposed to a mixture nanoscale polymer degradates, and other dissolved and volatile substances. The study highlights the fact that when the risks of polymer products in the environment are being assessed, we should not only consider the parent compound but also the products of the degradation process.

Other questions arising from this research include the characterisation of the types of dissolved and volatile substance that have been formed and the extent to which microbial activity influences degradation rate. While this study has focused on latex as a test material there is no reason why the approaches taken here cannot be applied to other materials.

## Acknowledgements

This study was funded by the Department for Environment Food and Rural Affairs (DEFRA), Seedcorn fund. We would also like to thank James Clark and Paul Elliot at the Green Chemistry Department, University of York and Sujung Park and Rebecca Sutton at the Environment Department; University of York for arranging access to analytical equipment.

## Appendix A. Supplementary data

Supplementary data to this article can be found online at http://dx.doi.org/10.1016/j.scitotenv.2012.12.067.

## References

Agamuthu P, Faizura PN. Biodegradability of degradable plastic waste. Waste Manag Res 2005;23:95-100.
Agostini DLS, Constantino CJL, Job AE. Thermal degradation of both latex and latex cast films forming membranes — combined TG/FTIR investigation. J Therm Anal Calorim 2008;91:703–7.
Albertsson AC, Andersson SO, Karlsson S. The mechanism of biodegradation of polyethylene. Polym Degrad Stab 1987;18:73–87.
Al-Salem SM. Influence of natural and accelerated weathering on various formulations of linear low density polyethylene (LLDPE) films. Mater Des 2009;30:1729–36.
Barnes DKA, Milner P. Drifting plastic and its consequences for sessile organism dispersal in the Atlantic Ocean. Mar Biol 2005;146:815–25.
Barnes DKA, Galgani F, Thompson RC, Barlaz M. Accumulation and fragmentation of plastic debris in global environments. Philos Trans R Soc B Sci 2009;364:1985–98.
Barnes DKA, Walters A, Goncalves L. Macroplastics at sea around Antarctica. Mar Environ Res 2010;70:250–2.
Bravo M, Gallardo MD, Luna-Jorquera G, Nunez P, Vasquez N, Thiel M. Anthropogenic debris on beaches in the SE Pacific (Chile): results from a national survey supported by volunteers. Mar Pollut Bull 2009;58:1718–26.
Cherian E, Jayachandran K. Microbial degradation of natural rubber latex by a novel species of *Bacillus* sp. SBS25 isolated from soil. Int J Environ Res 2009;3:599–604.
Cit I, Sinag A, Yumak T, Ucar S, Misirlioglu Z, Canel M. Comparative pyrolysis of polyolefins (PP and LDPE) and PET. Polym Bull 2010;64:817–34.
Cosgrove L, McGeechan PL, Robson GD, Handley PS. Fungal communities associated with degradation of polyester polyurethane in soil. Appl Environ Microbiol 2007;73:5817–24.
Desai MP, Labhasetwar V, Walter E, Levy RJ, Amidon GL. The mechanism of uptake of biodegradable microparticles in Caco-2 cells is size dependent. Pharm Res 1997;14:1568–73.
Dhawan A, Pandey A, Sharma V. Toxicity assessment of engineered nanomaterials: resolving the challenges. J Biomed Nanotechnol 2011;7:6–7.
Filipe V, Hawe A, Jiskoot W. Critical evaluation of nanoparticle tracking analysis (NTA) by NanoSight for the measurement of nanoparticles and protein aggregates. Pharm Res 2010;27:796–810.
FOCUS. Guidance document on estimating persistence and degradation kinetics from environmental fate studies on pesticides in EU Registration. Report of the FOCUS Work Group on Degradation Kinetics, EC Document Reference Sanco/10058/2005 version 2.0; 2006. [434 pp.].
Galgani F, Leaute JP, Moguedet P, Souplet A, Verin Y, Carpentier A, et al. Litter on the sea floor along European coasts. Mar Pollut Bull 2000;40:516–27.
Gillespie C, Halling P, Edwards D. Monitoring of particle growth at a low concentration of a poorly water soluble drug using the NanoSight LM20. Colloids Surf A Physicochem Eng Asp 2011;384:233–9.
Kaczmarek H, Bajer K, Galka P, Kotnowska B. Photodegradation studies of novel biodegradable blends based on poly(ethylene oxide) and pectin. Polym Degrad Stab 2007;92:2058–69.
Klemchuk PP. Degradable Plastics — a critical-review. Polym Degrad Stab 1990;27:183–202.
Krzan A, Hemjinda S, Miertus S, Corti A, Chiellini E. Standardization and certification in the area of environmentally degradable plastics. Polym Degrad Stab 2006;91:2819–33.
Linos A, Berekaa MM, Reichelt R, Keller U, Schmitt J, Flemming HC, et al. Biodegradation of cis-1,4-polyisoprene rubbers by distinct actinomycetes: microbial strategies and detailed surface analysis. Appl Environ Microbiol 2000;66:1639–45.
Lucas N, Bienaime C, Belloy C, Queneudec M, Silvestre F, Nava-Saucedo JE. Polymer biodegradation: mechanisms and estimation techniques. Chemosphere 2008;73:429–42.
Mailhot B, Morlat S, Gardette JL. Photooxidation of blends of polystyrene and poly(vinyl methyl ether): FTIR and AFM studies. Polymer 2000;41:1981–8.
Montes-Burgos I, Walczyk D, Hole P, Smith J, Lynch I, Dawson K. Characterisation of nanoparticle size and state prior to nanotoxicological studies. J Nanopart Res 2010;12:47–53.
Nagai N, Matsunobe T, Imai T. Infrared analysis of depth profiles in UV-photochemical degradation of polymers. Polym Degrad Stab 2005a;88:224–33.

Nagai Y, Nakamura D, Miyake T, Ueno H, Matsumoto N, Kaji A, et al. Photodegradation mechanisms in poly(2,6-butylenenaphthalate-co-tetramethyleneglycol) (PBN-PTMG). I: influence of the PTMG content. Polym Degrad Stab 2005b;88:251–5.
Nor HM, Ebdon JR. Ozonolysis of natural rubber in chloroform solution Part 1. A study by GPC and FTIR spectroscopy. Polymer 2000;41:2359–65.
O'Brine T, Thompson RC. Degradation of plastic carrier bags in the marine environment. Mar Pollut Bull 2010;60:2279–83.
Oigman-Pszczol SS, Creed JC. Quantification and classification of marine litter on beaches along Armacao dos Buzios, Rio de Janeiro, Brazil. J Coastal Res 2007;23:421–8.
Riyajan S, Sakdapipanich JT, Tanaka Y. Controlled degradation of cured natural rubber by encapsulated benzophenone as a photosensitizer. J Appl Polym Sci 2003;90: 297–305.
Rutkowska M, Heimowska A, Krasowska K, Janik H. Biodegradability of polyethylene starch blends in sea water. Pol J Environ Stud 2002a;11:267–71.
Rutkowska M, Krasowska K, Heimowska A, Steinka I, Janik H. Degradation of polyurethanes in sea water. Polym Degrad Stab 2002b;76:233–9.
Saad GR, Khalil TM, Sabaa MW. Photo- and bio-degradation of poly(ester-urethane)s films based on poly[(R)-3-Hydroxybutyrate] and poly(epsilon-Caprolactone) blocks. J Polym Res 2010;17:33–42.
Santos IR, Friedrich A, do Sul JAI. Marine debris contamination along undeveloped tropical beaches from northeast Brazil. Environ Monit Assess 2009;148:455–62.
Stefatos A, Charalampakis M, Papatheodorou G, Ferentinos G. Marine debris on the seafloor of the Mediterranean Sea: examples from two enclosed gulfs in western Greece. Mar Pollut Bull 1999;38:389–93.
Sudhakar M, Trishul A, Doble M, Kumar KS, Jahan SS, Inbakandan D, et al. Biofouling and biodegradation of polyolefins in ocean waters. Polym Degrad Stab 2007;92: 1743–52.
Tsuchii A, Suzuki T, Takeda K. Microbial-degradation of natural-rubber vulcanizates. Appl Environ Microbiol 1985;50:965–70.
Tsuchii A, Takeda K, Tokiwa Y. Degradation of the rubber in truck tires by a strain of Nocardia. Biodegradation 1997;7:405–13.